Nanopore detection of single-molecule binding within a metallosupramolecular cage

Nanopore Detection of Single-molecule Binding within a Metallosupramolecular Cage

Stefan Borsley,[a] James A. Cooper,[a] Paul J. Lusby[a] and Scott L. Cockroft*[a]

Abstract:

Guest encapsulation is a fundamental property of coordination cages. However, there is a paucity of methods capable of quantifying the dynamics of guest binding processes. Here, we demonstrate nanopore detection of single-molecule binding within metallosupramolecular cages. Real-time monitoring of the ion current flowing through a transmembrane α-hemolysin nanopore resolved the binding of different guests to both cage enantiomers. This enabled the single-molecule kinetics of guest binding to be quantified, while the ordering and durations of events were consistent with a guest-exchange mechanism that does not involve ligand dissociation. In addition to providing a new approach for single-molecule interrogation of dynamic supramolecular processes, we also established that cage complexes which are too large to enter the nanopore can be exploited for detecting small molecules, thus constituting a new class of molecular adapter.

Coordination chemistry provides access to a diverse range of supramolecular structures with remarkable properties.[1] For example, the ability of metallosupramolecular cages to bind guest molecules within an internal cavity has been widely exploited in molecular recognition and sensing,[2] gas separation,[3] stabilization of reactive species,[4] and catalysis.[4d, 5] This abundance of applications combined with the desire to incorporate more sophisticated functionalities into supramolecular assemblies necessitates the development of a fundamental, quantitative understanding of guest binding processes.[6] To date, such studies have largely employed ensemble techniques, such as NMR spectroscopy, to quantify the thermodynamic aspects of binding.[7] However, accessing kinetic parameters using ensemble techniques is often very challenging, especially where equilibration times are rapid.[6a, 6b, 6g, 6i, 8] In contrast, single-molecule techniques may provide a means of observing the real-time dynamics, distribution and ordering of processes occurring on the molecular level.[9]

Here, we examine the ability of the ion current flowing through a single α-hemolysin nanopore embedded in a lipid membrane to resolve the binding of single molecules within individual enantiomers of a metallosupramolecular cage (Figure 1). We recently established[10] that the experimental setup depicted in Figure 1A could be used to discriminate between the homochiral enantiomers of a $Ga^{III}_4L_6^{12-}$ tetrahedral coordination cage.[11] Therefore, we sought to explore whether the approach might be extended to resolve the dynamic encapsulation of guests within the transiently associated cage complexes (Figure 1). Such an approach would resemble the use of β-cyclodextrins,[13] cyclic peptides[14] and cucurbit[6]urils,[15] which have been used as supramolecular adapters in combination with the α-hemolysin nanopore to detect molecules that would otherwise be too small to attenuate the ion current flowing through the nanopore (Figure S25–S28). Such molecular adapters are deeply occluded, or even covalently bound within the lumen of the pore. In contrast, the cages shown in Figure 1B interact only transiently with the *cis*-opening of the pore and are too large to enter it (cage diameter = 2.5 nm, *cis*- nanopore entrance = 2.5 nm Figure S35).[10] Thus, it was not clear whether the molecular adapter principle could also be exploited in transiently associated complexes, particularly given the subtle changes that might be expected to arise from the association of a small guest molecule within a substantially larger and relatively rigid supramolecular cage.

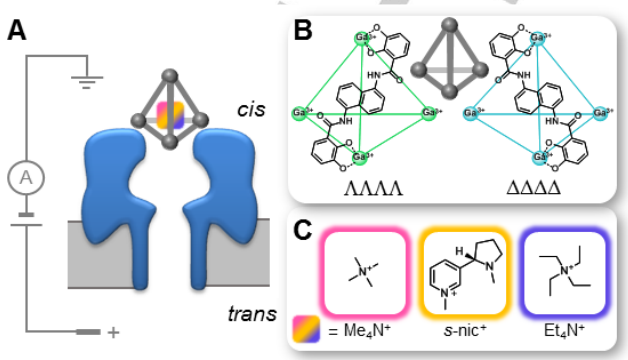

Figure 1. (**A**) Experimental setup in which tetrahedral coordination cages were detected at the *cis*-opening of a single α-hemolysin nanopore inserted in a lipid bilayer under an applied transmembrane potential. (**B**) ΛΛΛΛ (green) and ΔΔΔΔ (blue) homochiral forms of the $Ga^{III}_4L_6^{12-}$ cage used in this study. Each coloured edge indicates the position of a bridging ligand molecule. (**C**) Range of well-established[11-12] cationic guests employed in this study.

Initially, we synthesized a racemic mixture of the $Ga^{III}_4L_6^{12-}$ tetrahedral coordination cage (Figure 1B),[11] in the presence of a tetramethylammonium guest (Me_4N^+, Figure 1C, pink). ^{1}H NMR spectroscopy revealed that each cage was associated with one external Me_4N^+ and one encapsulated Me_4N^+ (Figure S3), in accordance with literature chemical shifts.[11] Nanopore experiments were conducted using a setup in which a planar lipid bilayer was painted across a 100 μm aperture separating two wells of buffered solution (1 M KCl, 30 mM phosphate, pH 8.0) (Figures S1, S2). A single α-hemolysin nanopore was introduced into the bilayer, as indicated by the characteristic ionic current flowing through the pore at an applied transmembrane voltage of +100 mV (I_o, Figure 2, S5). The addition of the Me_4N^+⊂cage complex to a final concentration of ~0.5 μM on the *cis*-side of the

[a] Dr S. Borsley, Dr J. A. Cooper, Dr P. J. Lusby and Dr S. L. Cockroft
EaStCHEM School of Chemistry
University of Edinburgh, Joseph Black Building
David Brewster Road, Edinburgh EH9 3FJ, UK
E-mail: scott.cockroft@ed.ac.uk

Supporting information for this article is given via a link at the end of the document.

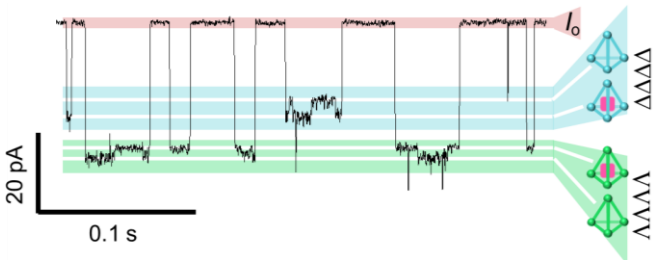

Figure 2. Representative ion current trace (1 M KCl, 30 mM phosphate, pH 8.0, +100 mV, 293 ± 2 K) in the presence of 0.5 μM $Ga^{III}_4L_6^{12-}$⊂Me_4N^+ on the *cis*-side of the bilayer. Extended ion traces are provided in Figures S6, S7. I_o is the free-pore current.

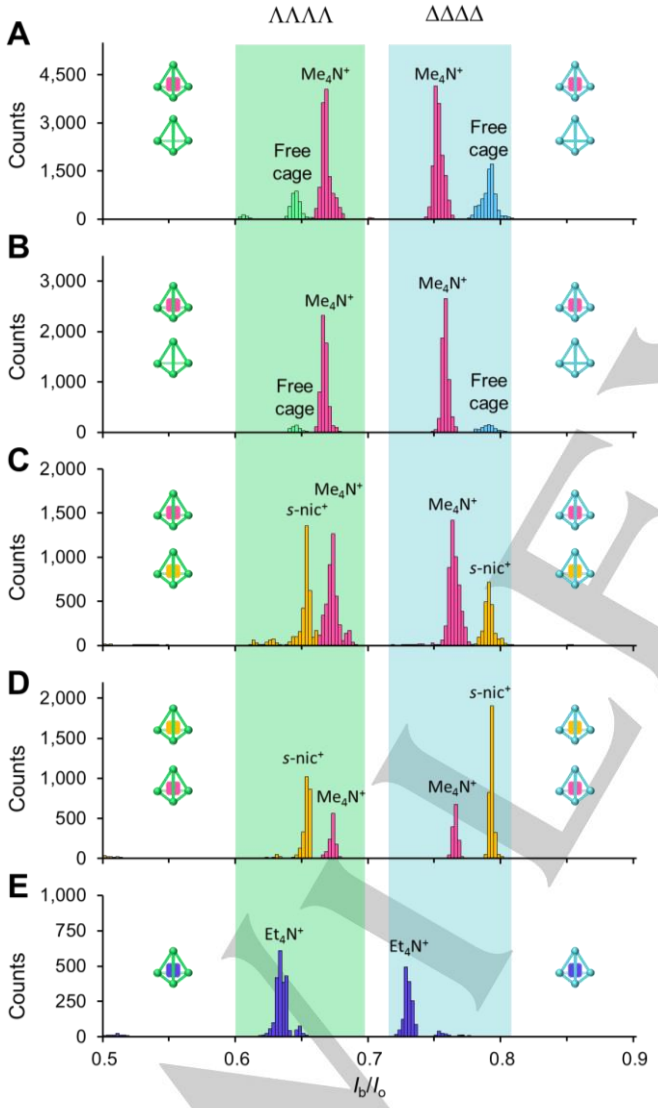

Figure 3. Histograms of the residual currents (1 M KCl, 30 mM phosphate, pH 8.0, +100 mV, 293 ± 2 K) observed across multiple titration experiments with components being successively added to the *cis*-side of the membrane. (**A**) [$Ga^{III}_4L_6^{12-}$] = 0.5 μM, [Me_4N^+] = 1.0 μM, (**B**) [$Ga^{III}_4L_6^{12-}$] = 0.5 μM, [Me_4N^+] = 9.3 μM, (**C**) [$Ga^{III}_4L_6^{12-}$] = 0.5 μM, [Me_4N^+] = 9.3 μM, [*s*-nic$^+$] = 1.6 μM, (**D**) [$Ga^{III}_4L_6^{12-}$] = 0.5 μM, [Me_4N^+] = 9.3 μM, [*s*-nic$^+$], 3.2 μM, (**E**) [$Ga^{III}_4L_6^{12-}$] = 0.5 μM, [Me_4N^+] = 9.3 μM, [*s*-nic$^+$] 3.2 μM, [Et_4N^+] 161 μM. Extended data provided in Figures S6–S20.

bilayer (Figure 1A) gave rise to temporal blockages of the ion current at two major levels (green and blue bars in Figure 2), corresponding to the two homochiral cage enantiomers (ΛΛΛΛ and ΔΔΔΔ).[10-11] Intriguingly, sub-levels were observed within these major bands that we reasoned may arise from exchange between the free cage and guest-encapsulated states (white lines, Figure 2).[16] Indeed, data collated from multiple experiments and consisting of several thousand blockage events revealed four discrete Gaussian event distributions that could be tentatively attributed to the two free cage enantiomers, and the two Me_4N^+⊂$Ga^{III}_4L_6^{12-}$ inclusion complexes (Figure 3A).

Changes in the event distributions as the concentration of Me_4N^+ was increased were used to assign the free and guest-bound cages (e.g. Figure 3A → 3B, and Figures S31–S32 for other concentrations). In contrast to the changes in the population of states induced by varying the concentration of Me_4N^+, there was no change in the magnitude of the residual currents of each state, indicating that the μM-concentration of non-encapsulated Me_4N^+ ions had a negligible influence on the ion current in the 1 M KCl buffer solution employed. We next added a second, competing guest to the experiment (*s*-nic$^+$, Figure 1C, yellow, Figure S4), which is known to bind more strongly to the cages.[12] Two new current levels were observed, which we attributed to the *s*-nic$^+$⊂$Ga^{III}_4L_6^{12-}$ complexes (Figure 3B → 3C, yellow). The relatively high population of new events despite the lower concentration of *s*-nic$^+$ compared to Me_4N^+ is also consistent with stronger binding of the chrial cationic guest. The addition of further *s*-nic$^+$ further increased the relative population of these new states, strongly indicating that these are attributable to the *s*-nic$^+$⊂$Ga^{III}_4L_6^{12-}$ complexes (Figure 3C → 3D). Finally, an excess of Et_4N^+ (Figure 1C, purple) was added, which is known to outcompete *s*-nic$^+$ binding within the cages.[6b] Accordingly, two new levels were observed corresponding to the near total formation of the Et_4N^+⊂$Ga^{III}_4L_6^{12-}$ complexes at the expense of all previously observed states (Figure 3D → 3E). Notably, the addition of *n*-Bu_4N^+ (Figures S21–S23) to a ~0.5 μM solution of the cage⊂Me_4N^+ complex did not generate any additional current levels (Figure 3A → S24). Since *n*-Bu_4N^+ has previously been shown to be too large to enter the cage, but may still interact via external electrostatic interactions,[17] such a finding is consistent with the hypothesis that the discrete current levels observed arise from the encapsulation of different guests within the cage complexes.

Interestingly, some encapsulated states increased the ion current relative to the free cage, while others diminished it. For example, Me_4N^+ binding within the ΛΛΛΛ cage increased the ion current, whereas Me_4N^+ binding within the ΔΔΔΔ cage decreased the ion current (Figure 3A and 3B). Conversely, Et_4N^+ binding resulted in a decrease in ion current relative to the empty cage for both ΛΛΛΛ and ΔΔΔΔ cages (Figure 3E). This observation underlines the non-intuitive nature of ion currents, which are difficult to predict.[18] Nonetheless, one may speculate that such differences might arise from subtle variations in the shapes, charge distributions, and/or solvation shells of each of the complexes, all of which are further modulated by the diastereomeric nature of the interactions with the pore.

One benefit of single-molecule approaches is that they can enable direct observation of association/dissociation events, and the distribution of kinetics relating to these individual events. Thus, having qualitatively established that guest binding within the

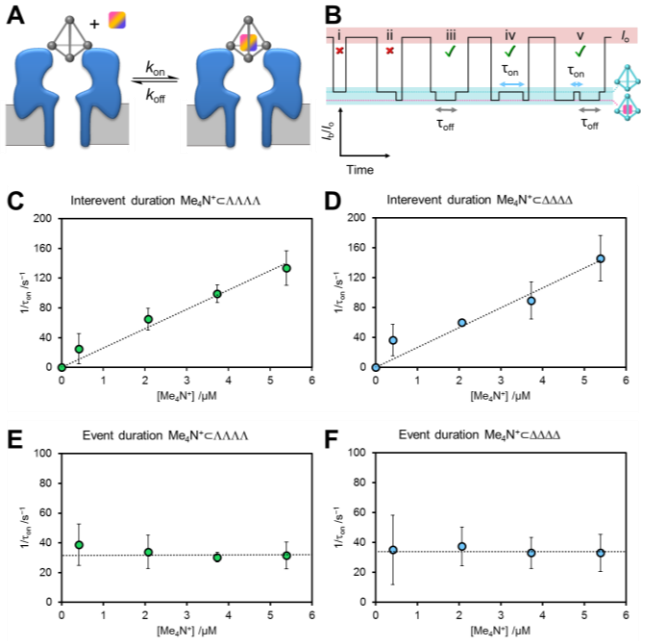

Figure 4. (**A**) Scheme showing guest kinetic parameters k_{on} and k_{off} for guest binding within a $Ga^{III}_4L_6^{12-}$ cage that is transiently associated with an α-hemolysin nanopore. (**B**) Illustration of event types from which guest binding durations (τ_{off}) and inter-event durations (τ_{on}) can be determined. (**C–F**) Experimental data showing association/dissociation kinetics of Me_4N^+ binding to ΛΛΛΛ and ΔΔΔΔ cages whilst transiently associated with an α-hemolysin nanopore as the concentration of Me_4N^+ is varied. [ΛΛΛΛ] = [ΔΔΔΔ] = 0.10 μM, 1 M KCl, 30 mM phosphate, pH 8.0, +100 mV, 293 ± 2 K. The rate constant k_{on} was obtained from the slope of the linear fit of $1/\tau_{on}$ versus [Me_4N^+] for (**C**) ΛΛΛΛ and (**D**) ΔΔΔΔ cages. The rate constant k_{off} was obtained from the intercept of the graph $1/\tau_{off}$ *versus* [Me_4N^+] for (**E**) ΛΛΛΛ and (**F**) ΔΔΔΔ cages.

cages could be differentiated, we sought to quantify the kinetics of guest binding at the single-molecule level (Figure 4A).[9] Such a kinetic analysis can only be performed when there are sufficient measurements of complete guest-binding durations (τ_{off}, Figure 4B, iii and v), and inter-event durations (τ_{on}, Figure 4B, iv and v) during the periods in which the cage is associated with the pore (Figure S29). The challenge with the present system is that cages are only transiently associated with the pore (half-life ~30 ms),[10] which limits the window in which cage-guest binding can be observed. Indeed, incomplete binding/unbinding events (Figure 4B, i and ii) must be disregarded in such an analysis. Since a complete kinetic analysis requires sufficient measurements across a range of guest concentrations, the aforementioned factors may make data collection time-consuming. Furthermore, longer guest-binding events may be under-represented (e.g. truncated bound state in Figure 4B, ii), which may limit the accuracy of the determined kinetic parameters.

Nonetheless, we proceeded to see whether it was possible to measure guest-binding kinetics at the single-molecule level. $Ga^{III}_4L_6^{12-}$⊂Me_4N^+ was added to a single nanopore experiment under an applied transmembrane voltage of +100 mV. Me_4N^+ was titrated into the experiment and single channel recordings obtained (Figure S30–S32). Event durations and interevent durations (τ_{off} and τ_{on} respectively, Figure 4B) were obtained and plotted as frequency-count histograms, which were fitted to single- exponential decay functions (Figure S33–S34) for each cage-enantiomer. For both cage enantiomers, τ_{off} was found to be

Table 1. Residual ion currents, kinetic and thermodynamic data for voltage-driven $Ga^{II}_4L_6$⊂Me_4N^+ complexation determined from nanopore experiments ([ΛΛΛΛ] = [ΔΔΔΔ] = 0.1 μM, 1 M KCl, 30 mM phosphate, pH 8.0, +100 mV, 293 ± 2 K). K_a is given by k_{on}/k_{off} for each cage complex.

	ΛΛΛΛ $Ga^{III}_4L_6^{12-}$⊂Me_4N^+	ΔΔΔΔ $Ga^{III}_4L_6^{12-}$⊂Me_4N^+
Residual current, I_b/I_o (free cage)	0.64 ± 0.003	0.79 ± 0.004
Residual current, I_b/I_o (⊂Me_4N^+)	0.67 ± 0.003	0.75 ± 0.005
Guest association, k_{on} /M^{-1} s^{-1}	2.61 ± 0.38 × 10^7	2.66 ± 0.39 × 10^7
Guest dissociation, k_{off} /s^{-1}	32 ± 2	34 ± 2
Non-equilibrium association constant at +100 mV, $K_{non\text{-}eq}$ /M^{-1}	8.3 ± 1.3 × 10^5	7.8 ± 1.2 × 10^5

independent of guest concentration, whereas τ_{on} was linearly dependent on concentration (Figure 4C–F). These concentration dependencies confirmed the bimolecular nature of guest encapsulation, and the unimolecular nature of guest expulsion with each cage enantiomer. Moreover, this indicated that the caveats outlined in the previous paragraph did not undermine the integrity of this approach for this host-guest combination. Thus, the voltage-driven rate constants of association, $k_{on} = 1/(\tau_{on}[Me_4N^+])$, and dissociation, $k_{off} = 1/\tau_{off}$, could be determined from the data in Figure 4C–F (Table 1). These experimentally determined k_{on} and k_{off} values were the same within error, indicating that the diastereotopic relationship between the cage and the nanopore does not affect the guest binding process. The ratio of k_{on}/k_{off} provides the association constant for guest binding within the cage ($K_{non\text{-}eq}$, Table 1).[19] Consistent with previous nanopore-based investigations of host-guest complexation,[13] these non-equilibrium association constants (measured under an applied potential of +100 mV) were found to be four orders of magnitude greater than the equivalent association constants measured at equilibrium.[11]

Notably, the single-molecule data presented herein supports the previously proposed non-dissociative mechanism in which all vertices of the cage remain intact during both guest entry and exit.[6b, 20] Specifically, the distributions of event and inter-event durations (τ_{off} and τ_{on}, respectively) follow single exponential decay functions (Figure S33–S34), and no intermediate states could be resolved between the guest-bound and free states on the low-millisecond timescale (Figures 2, S7, S10).

In conclusion, we have demonstrated a nanopore-based approach for detecting the binding of single molecules within individual metallosupramolecular cages. More specifically, the magnitude of the ion current blockages arising from the transient association of enantiomeric tetrahedral $Ga^{III}_4L_6^{12-}$ cages with an α-hemolysin protein nanopore allowed individual cage-guest complexes to be distinguished. The ability of this method to resolve subtle differences between cage enantiomers and cage-guest complexes is striking, particularly given that they are too large to enter the pore.[10] Thus, this approach extends the molecular adapter principle beyond established nanopore-detection strategies in which smaller adapters reside deep within the pore.[13-15] In common with other nanopore-based detection

methods, the non-equilibrium (voltage-driven) nature of the approach facilitates the detection of small molecules at sub-micromolar concentrations. Similarly, direct observation of guest binding within an individual cage grants access not only to thermodynamic data, but also hard-to-obtain single-molecule distributions of kinetic data. We hope that this work will encourage the use of nanopore-based approaches for gaining insights into other dynamic supramolecular systems, even where the structures are too large to enter the pore.

Experimental Section

Experimental Details are provided in the SI.

Acknowledgements

We thank ERC Starting Grant 336935, “Transmembrane molecular machines” for funding.

Keywords: single-molecule studies • supramolecular chemistry • cage compounds • sensors • molecular recognition

[1] a) G. F. Swiegers, T. J. Malefetse, *Chem. Rev.* **2000**, *100*, 3483-3538; b) B. J. Holliday, C. A. Mirkin, *Angew. Chem. Int. Ed.* **2001**, *40*, 2022-2043; *Angew. Chem.* **2001**, *113*, 2076-2097; c) R. Chakrabarty, P. S. Mukherjee, P. J. Stang, *Chem. Rev.* **2011**, *111*, 6810-6918; d) S. R. Seidel, P. J. Stang, *Acc. Chem. Res.* **2002**, *35*, 972-983; e) T. R. Cook, P. J. Stang, *Chem. Rev.* **2015**, *115*, 7001-7045.

[2] a) R. Custelcean, P. V. Bonnesen, N. C. Duncan, X. Zhang, L. A. Watson, G. Van Berkel, W. B. Parson, B. P. Hay, *J. Am. Chem. Soc.* **2012**, *134*, 8525-8534; b) Y. R. Hristova, M. M. J. Smulders, J. K. Clegg, B. Breiner, J. R. Nitschke, *Chem. Sci.* **2011**, *2*, 638-641; c) T. K. Ronson, A. B. League, L. Gagliardi, C. J. Cramer, J. R. Nitschke, *J. Am. Chem. Soc.* **2014**, *136*, 15615-15624; d) S. Turega, M. Whitehead, B. R. Hall, A. J. H. M. Meijer, C. A. Hunter, M. D. Ward, *Inorg. Chem.* **2013**, *52*, 1122-1132; e) C. García-Simón, M. Garcia-Borràs, L. Gómez, I. Garcia-Bosch, S. Osuna, M. Swart, J. M. Luis, C. Rovira, M. Almeida, I. Imaz, D. Maspoch, M. Costas, X. Ribas, *Chem. Eur. J.* **2013**, *19*, 1445-1456; f) C. García-Simón, M. Garcia-Borràs, L. Gómez, T. Parella, S. Osuna, J. Juanhuix, I. Imaz, D. Maspoch, M. Costas, X. Ribas, *Nat. Commun.* **2014**, *5*, 5557; g) P. D. Frischmann, V. Kunz, F. Würthner, *Angew. Chem. Int. Ed.* **2015**, *54*, 7285-7289; *Angew. Chem.* **2015**, *127*, 7393-7397; h) H. Takezawa, S. Akiba, T. Murase, M. Fujita, *J. Am. Chem. Soc.* **2015**, *137*, 7043-7046.

[3] a) M. B. Duriska, S. M. Neville, J. Lu, S. S. Iremonger, J. F. Boas, C. J. Kepert, S. R. Batten, *Angew. Chem. Int. Ed.* **2009**, *48*, 8919-8922; *Angew. Chem.* **2009**, *121*, 9081-9084; b) I. A. Riddell, M. M. J. Smulders, J. K. Clegg, J. R. Nitschke, *Chem. Commun.* **2011**, *47*, 457-459.

[4] a) S. Horiuchi, T. Murase, M. Fujita, *J. Am. Chem. Soc.* **2011**, *133*, 12445-12447; b) K. Nakabayashi, M. Kawano, M. Fujita, *Angew. Chem. Int. Ed.* **2005**, *44*, 5322-5325; *Angew. Chem.* **2005**, *117*, 5456-5459; c) P. Mal, B. Breiner, K. Rissanen, J. R. Nitschke, *Science* **2009**, *324*, 1697-1699; d) W. M. Hart-Cooper, K. N. Clary, F. D. Toste, R. G. Bergman, K. N. Raymond, *J. Am. Chem. Soc.* **2012**, *134*, 17873-17876.

[5] a) C. J. Brown, F. D. Toste, R. G. Bergman, K. N. Raymond, *Chem. Rev.* **2015**, *115*, 3012-3035; b) C. J. Hastings, M. D. Pluth, R. G. Bergman, K. N. Raymond, *J. Am. Chem. Soc.* **2010**, *132*, 6938-6940; c) Y. Jiao, J. Wang, P. Wu, L. Zhao, C. He, J. Zhang, C. Duan, *Chem. Eur. J.* **2014**, *20*, 2224-2231; d) T. Murase, S. Horiuchi, M. Fujita, *J. Am. Chem. Soc.* **2010**, *132*, 2866-2867; e) M. Otte, P. F. Kuijpers, O. Troeppner, I. Ivanović-Burmazović, J. N. H. Reek, B. de Bruin, *Chem. Eur. J.* **2013**, *19*, 10170-10178; f) D. Samanta, S. Mukherjee, Y. P. Patil, P. S. Mukherjee, *Chem. Eur. J.* **2012**, *18*, 12322-12329; g) C. García-Simón, R. Gramage-Doria, S. Raoufmoghaddam, T. Parella, M. Costas, X. Ribas, J. N. H. Reek, *J. Am. Chem. Soc.* **2015**, *137*, 2680-2687; h) D. Fiedler, H. van Halbeek, R. G. Bergman, K. N. Raymond, *J. Am. Chem. Soc.* **2006**, *128*, 10240-10252; i) D. H. Leung, R. G. Bergman, K. N. Raymond, *J. Am. Chem. Soc.* **2007**, *129*, 2746-2747; j) M. D. Pluth, R. G. Bergman, K. N. Raymond, *Science* **2007**, *316*, 85-88; k) M. D. Pluth, R. G. Bergman, K. N. Raymond, *Angew. Chem. Int. Ed.* **2007**, *46*, 8587-8589; *Angew. Chem.* **2007**, *119*, 8741-8743; l) C. J. Hastings, D. Fiedler, R. G. Bergman, K. N. Raymond, *J. Am. Chem. Soc.* **2008**, *130*, 10977-10983; m) M. D. Pluth, R. G. Bergman, K. N. Raymond, *J. Am. Chem. Soc.* **2008**, *130*, 11423-11429; n) Z. J. Wang, K. N. Clary, R. G. Bergman, K. N. Raymond, F. D. Toste, *Nat. Chem.* **2013**, *5*, 100-103.

[6] a) M. M. J. Smulders, S. Zarra, J. R. Nitschke, *J. Am. Chem. Soc.* **2013**, *135*, 7039-7046; b) A. V. Davis, D. Fiedler, G. Seeber, A. Zahl, R. van Eldik, K. N. Raymond, *J. Am. Chem. Soc.* **2006**, *128*, 1324-1333; c) C. G. P. Taylor, W. Cullen, O. M. Collier, M. D. Ward, *Chem. Eur. J.* **2017**, *23*, 206-213; d) S. Turega, W. Cullen, M. Whitehead, C. A. Hunter, M. D. Ward, *J. Am. Chem. Soc.* **2014**, *136*, 8475-8483; e) S. Mecozzi, J. J. Rebek, *Chem. Eur. J.* **1998**, *4*, 1016-1022; f) J. L. Bolliger, T. K. Ronson, M. Ogawa, J. R. Nitschke, *J. Am. Chem. Soc.* **2014**, *136*, 14545-14553; g) W. Jiang, D. Ajami, J. Rebek, *J. Am. Chem. Soc.* **2012**, *134*, 8070-8073; h) D. P. August, G. S. Nichol, P. J. Lusby, *Angew. Chem. Int. Ed.* **2016**, *55*, 15022-15026; *Angew. Chem.* **2016**, *128*, 15246-15250; i) O. Chepelin, J. Ujma, X. Wu, A. M. Z. Slawin, M. B. Pitak, S.J. Coles, J. Michel, A. C. Jones, P. E. Barran, P. J. Lusby, *J. Am. Chem. Soc.* **2012**, *134*, 19334-19337.

[7] C. Bohne, *Chem. Soc. Rev.* **2014**, *43*, 4037-4050.

[8] a) L. Avram, A. D. Wishard, B. C. Gibb, A. Bar-Shir, *Angew. Chem. Int. Ed.*, **2017**, *56*, 15314-15318; *Angew. Chem.*, **2017**, *129*, 15516-15520.

[9] L. Ma, S. L. Cockroft, *ChemBioChem* **2010**, *11*, 25-34.

[10] J. A. Cooper, S. Borsley, P. J. Lusby, S. L. Cockroft, *Chem. Sci.* **2017**, *8*, 5005-5009.

[11] D. L. Caulder, R. E. Powers, T. N. Parac, K. N. Raymond, *Angew. Chem. Int. Ed.* **1998**, *37*, 1840-1843; *Angew. Chem.* **1998**, *110*, 1940-1943.

[12] a) A. V. Davis, D. Fiedler, M. Ziegler, A. Terpin, K. N. Raymond, *J. Am. Chem. Soc.* **2007**, *129*, 15354-15363; b) A. J. Terpin, M. Ziegler, D. W. Johnson, K. N. Raymond, *Angew. Chem. Int. Ed.* **2001**, *40*, 157-160; *Angew. Chem.* **2001**, *113*, 161-164.

[13] a) L.-Q. Gu, O. Braha, S. Conlan, S. Cheley, H. Bayley, *Nature* **1999**, *398*, 686-690; b) J. Clarke, H.-C. Wu, L. Jayasinghe, A. Patel, S. Reid, H. Bayley, *Nat. Nanotechnol.* **2009**, *4*, 265-270; c) L.-Q. Gu, H. Bayley, *Biophys. J.* **2000**, *79*, 1967-1975.

[14] J. Sanchez-Quesada, M. R. Ghadiri, H. Bayley, O. Braha, *J. Am. Chem. Soc.* **2000**, *122*, 11757-11766.

[15] O. Braha, J. Webb, L.-Q. Gu, K. Kim, H. Bayley, *ChemPhysChem* **2005**, *6*, 889-892.

[16] Our previous work (see ref. 10), employed a Tris buffer, which binds strongly to the cages due to its close structural similarity to known cationic guests. Thus, current levels observed in the previous work likely arose from the $Ga^{III}_4L_6^{12-}\subset Tris\text{-}H^+$ complex.

[17] T. N. Parac, D. L. Caulder, K. N. Raymond, *J. Am. Chem. Soc.* **1998**, *120*, 8003-8004.

[18] S. F. Buchsbaum, N. Mitchell, H. Martin, M. Wiggin, A. Marziali, P. V. Coveney, Z. Siwy, S. Howorka, *Nano Lett.* **2013**, *13*, 3890-3896.

[19] Unfortunately, a similar analysis could not be performed for the *s*-nic$^+$ guest, as the residual current levels were coincident with the empty cage (*cf.* Figure 3A and 3D).

[20] A. V. Davis, K. N. Raymond, *J. Am. Chem. Soc.* **2005**, *127*, 7912-7919.

COMMUNICATION

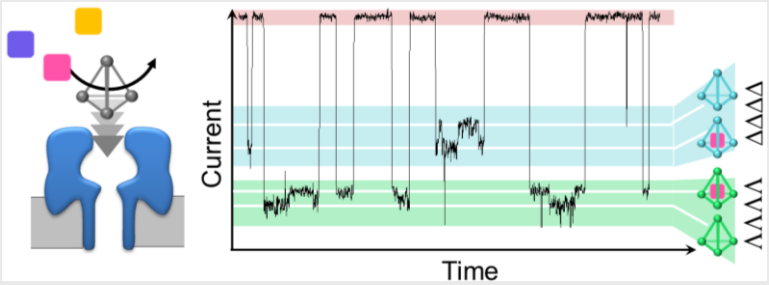

*Stefan Borsley, James A. Cooper, Paul J. Lusby and Scott L. Cockroft**

Page No. – Page No.

Nanopore detection of single-molecule binding within a metallosupramolecular cage

Be my guest: A protein nanopore can resolve both the chirality of individual metallosupramolecular cages, and the dynamics of encapsulation of different guests at the single-molecule level.